

A Bethe-Salpeter model for light mesons: spectra and decays

C.R.Münz, J.Resag, B.C.Metsch, H.R.Petry
*Institut für Theoretische Kernphysik,
Universität Bonn, Nussallee 14-16, 53115 Bonn, FRG*
(October 11, 2018)

The spectra and electroweak decay properties of light mesons are analyzed within the framework of the instantaneous Bethe-Salpeter equation. The interaction kernel comprises alternative spin-structures for a parameterization of confinement and a residual quark-antiquark interaction based on instanton effects. It is shown that only with a vector confinement the parameters can be chosen such as to yield an excellent description of the light pseudoscalar and vector mesons including weak and two photon decays. However it is found that it is not possible to reconcile this with the Regge behavior of higher lying meson states with the same parameter set.

I. INTRODUCTION

In a previous paper [1] it has been shown that the Bethe-Salpeter(BS) equation with an instantaneous interaction (Salpeter equation) provides a suitable framework for relativistic quark models of light mesons. The use of the Salpeter equation has several advantages compared to other treatments, i.e.

- The relativistic kinematics of the quarks is treated correctly;
- The amplitudes have the correct relativistic normalization;
- The lower component Φ^{--} of the Salpeter amplitude is determined dynamically.

On the other hand the practical advantages of a nonrelativistic treatment are also present, i.e.

- The Salpeter equation can be formulated as an eigenvalue problem $\mathcal{H}\psi = M\psi$ for the mass M of the bound state.
- One can define a (not positive definite) scalar product $\langle\psi_a|\psi_b\rangle$ for the Salpeter amplitudes.
- The Salpeter operator \mathcal{H} is selfadjoint with respect to this scalar product.

In [1] we have developed a numerical scheme which enables the calculation of meson mass spectra and the corresponding BS-amplitudes. Furthermore we have given formulas to compute some important electroweak meson decay widths.

In the present paper we shall apply this method to an explicit quark model for light mesons. Our main concern in this context will be whether a realistic description of deeply bound states like the pion is compatible with a reasonable description of confinement.

Let us first give a list of the main features of light mesons that will be considered in the following:

- the low masses of π and K
- the weak decay constants f_π and f_K
- the decays $\pi^0, \eta, \eta' \rightarrow 2\gamma$
- the masses and the flavor mixing coefficients of η and η'
- the masses and the leptonic decay widths for the ρ, ω and ϕ mesons
- the Regge behavior $M^2 \sim J$

As far as we know there presently is no model that can describe all these features in a consistent way. On the one hand there is the nonrelativistic quark model that gives a reasonable description of the mass spectra [2], but that completely fails in describing the decay widths of the deeply bound states like the pion (see Sec.IV D). On the other hand there are models like the Nambu Jona-Lasinio model [3–5] that are based on the chiral symmetry of QCD for vanishing current quark masses. This model leads to a good description for the π, K, η and η' mesons, but higher angular momenta states or radial excitations cannot be described since confinement is ignored.

An attempt to arrive at a more complete description based on the Salpeter equation has recently been given by J.F.Lagaë [6]. His results show the difficulty of finding a suitable ansatz for the confining interaction kernel: he rejects the hypothesis of an instantaneous scalar confining kernel.

The model we present in the following is based on a linear scalar or alternatively vector confining kernel combined with an effective interaction computed by 't Hooft from instanton effects in QCD [7–9]. A nonrelativistic version of this interaction has already lead to good results for the meson and baryon mass spectra [2]. We therefore feel encouraged to test this ansatz in the relativistic Bethe-Salpeter framework.

The paper is organized as follows: In Sec.II we briefly summarize the main features of the Salpeter equation as given in ref. [1]. The explicit form of the confining BS-kernel and of the 't Hooft kernel is given in Sec.III.

In Sec.IV we present the calculated meson mass spectra and obtain the pion and kaon decay constants f_π , f_K , the decay width into two photons for the π^0 , η and η' mesons and the leptonic widths for the vector mesons ρ , ω and ϕ . We will compare these decay widths to corresponding nonrelativistic results in Sec.IV D using the wave function of ref. [2], which shows the impressive improvement due to the relativistic treatment of the quarks compared to the nonrelativistic potential model. Finally we give some concluding remarks in Sec.V.

II. THE SALPETER EQUATION

For an instantaneous BS-kernel and free quark propagators the p^0 integrals in the BS-equation can be computed analytically in the rest frame of the bound state with mass M . The result is known as the Salpeter equation which reads

$$\begin{aligned} \Phi(\vec{p}) = & \int \frac{d^3 p'}{(2\pi)^3} \frac{\Lambda_1^-(\vec{p}) \gamma^0 [V(\vec{p}, \vec{p}') \Phi(\vec{p}')] \gamma^0 \Lambda_2^+(-\vec{p})}{M + \omega_1 + \omega_2} \\ & - \int \frac{d^3 p'}{(2\pi)^3} \frac{\Lambda_1^+(\vec{p}) \gamma^0 [(V(\vec{p}, \vec{p}') \Phi(\vec{p}')] \gamma^0 \Lambda_2^-(-\vec{p})}{M - \omega_1 - \omega_2} \quad (1) \end{aligned}$$

with $\omega_i = \sqrt{\vec{p}^2 + m_i^2}$, $\Lambda_i^\pm(\vec{p}) = (\omega_i \pm H_i(\vec{p})) / (2\omega_i)$ and $H_i(\vec{p}) = \gamma^0(\vec{\gamma}\vec{p} + m_i)$.

This equation can be reformulated into an eigenvalue problem for the bound state mass M . With the definitions

$$\psi(\vec{p}) := \Phi(\vec{p}) \gamma^0 \quad (2)$$

$$[W(\vec{p}, \vec{p}') \psi(\vec{p}')] := \gamma^0 [V(\vec{p}, \vec{p}') \Phi(\vec{p}')] \quad (3)$$

the Salpeter equation can now be written as

$$\begin{aligned} \mathcal{H}\psi &= M\psi \quad \text{with} \\ \mathcal{H}\psi &= H_1\psi - \psi H_2 \\ & - \int' \{ \Lambda_1^+ [W\psi'] \Lambda_2^- - \Lambda_1^- [W\psi'] \Lambda_2^+ \} \quad (4) \end{aligned}$$

with all quantities depending on \vec{p} or \vec{p}' (indicated with a prime) and the notation $\int' = \int d^3 p' / (2\pi)^3$.

One can now define a (not positive definite) scalar product for amplitudes $\psi_1 = \Phi_1 \gamma^0$ and $\psi_2 = \Phi_2 \gamma^0$ as

$$\langle \psi_1 | \psi_2 \rangle = \int \text{tr} \left(\psi_1^\dagger \Lambda_1^+ \psi_2 \Lambda_2^- - \psi_1^\dagger \Lambda_1^- \psi_2 \Lambda_2^+ \right) \quad (5)$$

The normalization condition for solutions of the Salpeter equation is then given as $\langle \psi | \psi \rangle = (2\pi)^2 2M$. If one considers amplitudes satisfying $\Lambda_1^+ \psi \Lambda_2^+ = \Lambda_1^- \psi \Lambda_2^- = 0$ one easily finds

$$\begin{aligned} \langle \psi_1 | \mathcal{H} \psi_2 \rangle &= \int (\omega_1 + \omega_2) \text{tr} \left(\psi_1^\dagger \psi_2 \right) \\ & - \int \int' \text{tr} \left(\psi_1^\dagger W \psi_2' \right) \quad (6) \end{aligned}$$

For most kernels of physical interests \mathcal{H} is selfadjoint with respect to the scalar product given above which implies that bound state masses M are real for eigenfunctions ψ with nonzero norm and that amplitudes ψ_1 and ψ_2 corresponding to different eigenvalues $M_1 \neq M_2^*$ are orthogonal, i.e. $\langle \psi_1 | \psi_2 \rangle = 0$.

III. THE BETHE-SALPETER KERNEL

A. Confinement

Up to now the confining interaction of QCD is only known in the static limit of heavy quarks. In this limit it has been shown [10,11] that the static potential between quarks is of the form $V_C(r) = a_c + b_c r + W$ where W denotes the relativistic corrections of the order p^2/m^2 . As stated by Gromes [10] it is still an open question whether an additional $1/r$ term should also be included into the static confining potential. Usually one concludes from the sign of the spin-orbit coupling term in W that the confining $q\bar{q}$ -interaction behaves like a Lorentz scalar.

The problem for the case of light quarks is that up to now there is no unambiguous extension of the confining potential beyond the static limit. Especially there is no prescription on how to extend it to a noninstantaneous form. Naive noninstantaneous extensions fail as has been shown by S.N.Biswas et al. [12] for the harmonic oscillator BS-kernel $V(x) = -bx^2 = b(\vec{x}^2 - (x^0)^2)$ that yields only a continuous spectrum. Similar results are to be expected for other kernels like $1/q^4$. Because of these difficulties the only way we see at the moment is to parameterize confinement as an instantaneous interaction kernel.

The sign of the LS-term in the static limit would be compatible with a scalar confinement kernel. However some authors [6,13] have shown that the linear Regge behavior $M^2 \sim J$ is lost for this choice, since bound state masses come out too small for higher angular momenta. This is due to the relativistic corrections to the static potential and becomes more problematic with decreasing quark masses. For a vector confining kernel this problem almost disappears, but in the static limit a vector kernel leads to an LS-term which has the wrong sign. To our knowledge there presently is no convincing parameterization for the confining kernel that exhibits both features, i.e. leads to linear Regge trajectories and yields a spin-orbit term with the correct sign.

In the following we will analyze both spin structures for the confinement, i.e. a scalar $1 \otimes 1$ and a vector $\gamma^0 \otimes \gamma_0$ interaction. In the rest frame of the bound state the corresponding BS-kernels in eq.(1) are parameterized as

$$[V_C^V(\vec{p}, \vec{p}') \Phi(\vec{p}')] = -\mathcal{V}_C((\vec{p} - \vec{p}')^2) \gamma^0 \Phi(\vec{p}') \gamma^0 \quad (7)$$

$$[V_C^S(\vec{p}, \vec{p}') \Phi(\vec{p}')] = \mathcal{V}_C((\vec{p} - \vec{p}')^2) \Phi(\vec{p}') \quad (8)$$

where \mathcal{V}_C is a scalar function which has the fourier transform $\mathcal{V}_C^F(r) = a_c + b_c r$.

B. 't Hooft interaction

1. The 't Hooft lagrangian

It is already known from nonrelativistic potential models that the masses of the scalar and pseudoscalar mesons π , K , η , η' cannot be described with a confining potential alone. The usual extension would be to add another contribution to the interaction kernel that comes from a One Gluon Exchange (OGE). This works quite well for heavy quarkonia [13,14], but it is highly questionable for light mesons where perturbation theory cannot be expected to work. Since OGE leads to a flavor independent interaction kernel one thus obtains degenerate π and η mesons in clear contradiction to the experimental mass values $m_\pi = 140 \text{ MeV}$ and $m_\eta = 549 \text{ MeV}$. In order to cure this discrepancy one would have to take into account higher order diagrams.

However there is another QCD based candidate for a residual $q\bar{q}$ -interaction computed by 't Hooft and others from instanton effects [7–9] which leads to good results for meson and baryon mass spectra within a nonrelativistic potential model [2].

Instantons are special solutions of the classical non-abelian Yang-Mills equations in Euclidian space. They are peaked both in space and imaginary time having a finite extension ρ . Since they cannot be deformed continuously into classical solutions corresponding to gluon fields they lead to an effective interaction between quarks that is not covered by perturbative gluon diagrams. This interaction leads to spontaneous breaking of chiral symmetry as can be seen by normal ordering of the underlying Lagrangian (see appendix A). The normal ordered Lagrangian takes the form

$$\mathcal{L} = k + \sum_{j=1}^3 : (i\bar{q}_j \gamma^\mu \partial_\mu q_j - m_j \bar{q}q) : + \Delta\mathcal{L}(2) + \Delta\mathcal{L}(3) \quad (9)$$

where k is an inessential constant that renormalizes the vacuum energy. $\Delta\mathcal{L}(2)$ and $\Delta\mathcal{L}(3)$ are two and three body terms and $m_j = m_j^0 + \Delta m_j$ is the effective constituent quark mass. In the following we will consider these terms.

2. The constituent quark mass

The contribution Δm_j to the effective constituent quark mass $m_j = m_j^0 + \Delta m_j$ is given by

$$\begin{aligned} \Delta m_n &= \int_0^{\rho_c} d\rho \frac{d_0(\rho)}{\rho^5} \frac{4}{3} \pi^2 \rho^3 \left(m_n^0 \rho - \frac{2}{3} \pi^2 \rho^3 \langle \bar{q}_n q_n \rangle \right) \\ &\quad \cdot \left(m_s^0 \rho - \frac{2}{3} \pi^2 \rho^3 \langle \bar{q}_s q_s \rangle \right) \\ \Delta m_s &= \int_0^{\rho_c} d\rho \frac{d_0(\rho)}{\rho^5} \frac{4}{3} \pi^2 \rho^3 \left(m_n^0 \rho - \frac{2}{3} \pi^2 \rho^3 \langle \bar{q}_n q_n \rangle \right)^2 \quad (10) \end{aligned}$$

where the instanton density for three colors and three flavors reads [15]

$$d_0(\rho) = (3.63 \cdot 10^{-3}) \left(\frac{8\pi^2}{g^2(\rho)} \right)^6 \exp \left(-\frac{8\pi^2}{g^2(\rho)} \right) \quad (11)$$

with

$$\left(\frac{8\pi^2}{g^2(\rho)} \right) = 9 \ln \left(\frac{1}{\Lambda_{QCD} \rho} \right) + \frac{32}{9} \ln \ln \left(\frac{1}{\Lambda_{QCD} \rho} \right) \quad (12)$$

within two loop accuracy [16]. Here Λ_{QCD} is the QCD scale parameter. The integration over the instanton size ρ has to be carried out up to a cutoff value ρ_c where the $\ln \ln$ term coming from the two loop correction is still small compared to the \ln term.

Equations (10) are usually called Gap equations. They describe the generation of a dynamical quark mass due to the interaction with the negative Dirac sea. In our model the constituent quark masses m_j will be used as free parameters that are fitted to the experimental data. It will be checked in the end (see Sec.IV E) whether the obtained quark masses are compatible with common values for the quark condensates present in Δm_j assuming that the confinement interaction does not contribute essentially to the process of chiral symmetry breaking.

3. The two body interaction

The two body term reads (see appendix A)

$$\begin{aligned} \Delta\mathcal{L}(2) &= -\frac{3}{16} \sum_i \sum_{kl} \sum_{mn} g_{\text{eff}}(i) \varepsilon_{ikl} \varepsilon_{imn} \\ &\quad \left\{ : q_k^\dagger q_l^\dagger [\gamma_0 \cdot \gamma_0 + \gamma_0 \gamma_5 \cdot \gamma_0 \gamma_5] (2\mathcal{P}_3^C + \mathcal{P}_6^C) q_m q_n : \right\} \quad (13) \end{aligned}$$

where the effective coupling constants are given as

$$g_{\text{eff}}(i) = \int_0^{\rho_c} d\rho \frac{d_0(\rho)}{\rho^5} \left(\frac{4}{3} \pi^2 \rho^3 \right)^2 \left(m_i^0 \rho - \frac{2}{3} \pi^2 \rho^3 \langle \bar{q}_i q_i \rangle \right) \quad (14)$$

and the tensor notation

$$q^\dagger q^\dagger (A \cdot B) q q := \sum_{i,j} \sum_{k,l} q_i^\dagger q_j^\dagger A_{ik} \cdot B_{jl} q_k q_l \quad (15)$$

has been used for Dirac and color indices. This representation explicitly shows the antisymmetric flavor dependence of the interaction. The color sextett and antitriplett projection matrices are given by

$$\mathcal{P}_6^C = \frac{1}{2}(1^C + \Pi^C) = \frac{2}{3}1^C + \frac{1}{4}\vec{\lambda}\cdot\vec{\lambda} \quad (16)$$

$$\mathcal{P}_3^C = \frac{1}{2}(1^C - \Pi^C) = \frac{1}{3}1^C - \frac{1}{4}\vec{\lambda}\cdot\vec{\lambda} \quad (17)$$

so that

$$2\mathcal{P}_3^C + \mathcal{P}_6^C = \frac{1}{2}(31^C - \Pi^C) = \frac{4}{3}1^C - \frac{1}{4}\vec{\lambda}\cdot\vec{\lambda} \quad (18)$$

where Π^C is a color exchange matrix defined as $\Pi_{ij,kl}^C = \delta_{il}\delta_{jk}$ and λ^a ($a = 1, \dots, 8$) are the color matrices. Just like the quark masses also the coupling constants will be treated as free parameters in our model.

4. The three body interaction

After a lengthy calculation the three body force can finally be written in the form

$$\begin{aligned} \Delta\mathcal{L}(3) = & \frac{27}{80}g_{\text{eff}}^{(3)} \left\{ : q^\dagger q^\dagger q^\dagger \right. \\ & [\gamma_0 \cdot \gamma_0 \cdot \gamma_0 + \gamma_0 \gamma_5 \cdot \gamma_0 \gamma_5 \cdot \gamma_0 \\ & \left. + \gamma_0 \gamma_5 \cdot \gamma_0 \cdot \gamma_0 \gamma_5 + \gamma_0 \cdot \gamma_0 \gamma_5 \cdot \gamma_0 \gamma_5] \right. \\ & \left. \mathcal{P}_1^F (2\mathcal{P}_{10}^C + 5\mathcal{P}_8^C) qq q : \right\} \quad (19) \end{aligned}$$

where \mathcal{P}_1^F is the projector onto a three-particle flavor singulett state, \mathcal{P}_{10}^C and \mathcal{P}_8^C are projectors onto the color decuplett and the color octett. The effective three-body coupling constant is given by

$$g_{\text{eff}}^{(3)} = \int_0^{\rho_c} d\rho \frac{d_0(\rho)}{\rho^5} \left(\frac{4}{3}\pi^2 \rho^3 \right)^3 \quad (20)$$

Obviously this three body force does not contribute to $q\bar{q}$ -states and to colorfree qqq -states.

5. The 't Hooft kernel

In order to distinguish different indices in the following we will use the notation s_i for Dirac indices, c_i for color indices and f_i for flavor indices. The vertex corresponding to $\Delta\mathcal{L}_2$ is shown in Fig.1. The vertex reads

$$\begin{aligned} (-i) G_{f_3 f_4, f_1 f_2} (1_{s_3 s_1} 1_{s_4 s_2} + \gamma_{s_3 s_1}^5 \gamma_{s_4 s_2}^5) \\ (4/3 1_{c_3 c_1} 1_{c_4 c_2} - 1/4 \vec{\lambda}_{c_3 c_1} \cdot \vec{\lambda}_{c_4 c_2}) \quad (21) \end{aligned}$$

with the definition

$$G_{f_3 f_4, f_1 f_2} := \frac{3}{8} \sum_{f_5} g_{\text{eff}}(f_5) \epsilon_{f_5 f_3 f_4} \epsilon_{f_5 f_1 f_2} \quad (22)$$

For the $q\bar{q} \rightarrow q\bar{q}$ amplitude we have to consider the two diagrams given in Fig.2. In a meson the quark and the antiquark are in a color singulett state represented by the matrix $\chi_{c_1 c_2}^C = \delta_{c_1 c_2} / \sqrt{3}$. The color matrix elements for the two vertices are then given by

$$\sum_{c_1 c_2} \sum_{c_3 c_4} (\chi_{c_3 c_4}^C)^* \frac{1}{2} (3 1_{c_3 c_1} 1_{c_2 c_4} - \Pi_{c_3 c_2, c_1 c_4}) \chi_{c_1 c_2}^C = 0 \quad (23)$$

$$\sum_{c_1 c_2} \sum_{c_3 c_4} (\chi_{c_3 c_4}^C)^* \frac{1}{2} (3 1_{c_3 c_4} 1_{c_2 c_1} - \Pi_{c_3 c_2, c_4 c_1}) \chi_{c_1 c_2}^C = 4 \quad (24)$$

so that only the second vertex in Fig.2 contributes to the interaction kernel. The effective 't Hooft interaction vertex between $q\bar{q}$ color singulett states is then given by

$$(-4i) G_{f_2 f_3, f_1 f_4} (1_{s_3 s_4} 1_{s_2 s_1} + \gamma_{s_3 s_4}^5 \gamma_{s_2 s_1}^5) \quad (25)$$

Since we assume $SU(2)$ -flavor invariance of the interaction we set

$$g := \frac{3}{8}g_{\text{eff}}(s) \quad , \quad g' := \frac{3}{8}g_{\text{eff}}(n) \quad (26)$$

where s stands for strange and n stands for nonstrange (u,d) flavor. The results for $G_{f_2 f_3, f_1 f_4}$ are given in Tab.I. Tab.II shows the matrix elements of $G_{f_2 f_3, f_1 f_4}$ for the flavor functions

$$\pi^0 = (u\bar{u} - d\bar{d})/\sqrt{2} \quad (27)$$

$$\eta_n = (u\bar{u} + d\bar{d})/\sqrt{2} \quad (28)$$

$$\eta_s = s\bar{s} \quad (29)$$

From the vertex we can extract the lowest order contribution of the 't Hooft interaction to the BS-kernel as

$$\begin{aligned} [V_T(\vec{p}, \vec{p}') \Phi(\vec{p}')]_{f_1 f_2} = 4 \sum_{f'_1 f'_2} G_{f_2 f'_1, f_1 f'_2} \\ [1 \text{tr} (\Phi_{f'_1 f'_2}(\vec{p}')) + \gamma^5 \text{tr} (\Phi_{f'_1 f'_2}(\vec{p}') \gamma^5)] \quad (30) \end{aligned}$$

As shown in the appendix this interaction only acts on the scalar and pseudoscalar mesons $J^{\pi P} = 0^\pm$. For the pseudoscalar mesons it is attractive for the π with a coupling constant g and for the K with a coupling constant g' . For the η and η' the interaction leads to mixing of nonstrange and strange flavor amplitudes. The effective sign of the interaction is reversed for the scalar mesons thus being repulsive for the a_0 . Note that in the nonrelativistic limit the 't Hooft interaction only acts on the pseudoscalar states $J^{\pi P} = 0^-$. The 't Hooft kernel as it stands represents a pointlike interaction that has to be regularized. Following ref. [2] we do this by multiplying the kernel with a regularizing Gaussian function

$$\mathcal{V}_{\text{reg}}(q) = e^{-\frac{1}{4}\Lambda^2 q^2} \quad (31)$$

with $\vec{q} = \vec{p} - \vec{p}'$ and $q = |\vec{q}|$. In coordinate space this choice corresponds to replacing the $\delta(\vec{r})$ function by

$$\mathcal{V}_{\text{reg}}^F(r) = \frac{1}{(\Lambda\sqrt{\pi})^3} e^{-\frac{r^2}{\Lambda^2}} \quad (32)$$

which introduces a finite effective range Λ .

IV. RESULTS AND DISCUSSION

A. Models and Parameters

The main concern of our work was to see whether we can obtain a consistent description of a) the masses and decays of the low lying pseudoscalar and vector mesons and b) confinement reflected e.g. by the Regge trajectories.

For this purpose we investigate two different models of the confinement kernel: 1) a vector $\gamma^0 \otimes \gamma^0$ - and 2) a scalar $1 \otimes 1$ -structure.

The parameters used are the nonstrange and strange quark masses m_n and m_s , the offset a_c and slope b_c of the confinement interaction, the two coupling constants g , g' and the effective range Λ of the residual instanton induced interaction. So the total number of parameters amounts to seven.

We used two sets of parameters in the vector confinement case: Model V1 was tuned to reproduce the masses and decays of the low lying mesons. We therefore used a small nonstrange quark mass m_n , as the correct description of the pseudoscalar decays depends essentially on this quantity. Given this mass we had to take a moderate confinement slope to reproduce the decays of the vectormesons. The offset a_c was fixed by the ρ -mass and m_s by the K^* -mass. Finally g and g' were fixed by the masses of the pseudoscalars π, η and K . In Model V2 we used a larger nonstrange mass of m_n of about 1/3 of the nucleon mass, which is a value common to Nonrelativistic Quark Models. The aim of this parameter set was to obtain a good description of the Regge trajectories and the higher lying resonances.

Finally in Model S we investigated a scalar confinement provided with the same quark mass m_n as in V2. For this kernel it turned out that our method of solving this type of BS equation works reasonably for higher angular momenta only if the fraction of the confinement slope b_c and the quark mass m_q is sufficiently small. The parameters for the three model are listed in Tab.III.

B. Mass spectra

The quality of the mass spectra is different for the three models, as different priorities led us to the parameters. Common to all three models is an overall agreement of the masses of the pseudoscalars π, K, η, η' and the vector mesons ρ, ω, ϕ, K^* . The spectra for these meson are compared to experiment in Figs. 3,4. The 't Hooft interaction leads to the correct splitting of π, η and η' mass. In contrast with experiment, where the a^0 and f^0 are nearly degenerate, we obtain a large splitting due to the instanton induced interaction of several hundred MeV (compare Tab.IV). For a vector type kernel with positive spin orbit splitting this leads an enormous attraction: although there is a scalar state at roughly 1GeV, we also find a

state with imaginary mass and zero norm. The physical interpretation of this phenomenon however is not clear. For a scalar confinement this effect is compensated by the negative spin orbit splitting. In the following we will discuss the differences of the three parameter sets.

Since in model V1 we used a small confinement slope to reproduce the decays of the vectormesons, the calculated Regge trajectory is too flat (see Fig.5). The spin orbit splitting between the 1^{++} and 2^{++} mesons in our model is purely due to the confining interaction. In both models with vector kernel it is of order of 200 MeV exceeding the experimental mass difference, which is in fact rather small (see Tab.IV).

In model V2 with large quark masses and large confinement slope b_c we obtain a good description of the masses of all mesons comparable to the results in nonrelativistic calculations. However b_c has to be much larger in the BS framework, as obviously the kinetic energy is overestimated in nonrelativistic calculations. The Regge trajectories representing the confinement property are well reproduced (Fig.5). For the spin orbit splitting the same remarks as for V1 apply.

Finally model S shows a reasonable description of the ground states of the pseudoscalar and vector mesons. For the states with large angular momentum the method of solving the BS equation by a basis expansion does not lead to convergent solutions with positive norm. With increasing dimension of the basis the smallest positive eigenvalue decreases until it becomes imaginary (a similar problem arises if one studies a $\gamma_\mu \otimes \gamma^\mu$ interaction). We therefore cannot explicitly exclude a scalar confining potential, mainly because with the present parameters we were not able to find stationary solutions for higher angular momenta. For these reasons we also omitted in the Regge plot the state with angular momentum $j=4$. The f_1 meson mass is larger than the mass of the f_2 meson. Taken together with the results for the vector case this indicates that the spin orbit splitting can only be explained by a mixture of scalar and vector type interaction.

C. Decay Observables

In this section we will discuss the influence of the parameters on the decay observables of the pseudoscalar and vector mesons.

The parameters of Model V1 have been chosen in order to give a good description of the masses and the decays of the pseudoscalar and vector ground states. As can be seen in Tab.V, we obtain an almost quantitative agreement. As an important result we consider the fact that the π and η , which usually are interpreted as Goldstone particles of the of chiral symmetry breaking, also may be understood as bound states of quark and antiquark, albeit with relatively small quark masses. This is reflected in the simultaneous agreement we obtain for the pion de-

cay constant f_π and the decay width $\pi^0 \rightarrow \gamma\gamma$, which in the alternative Goldstone picture are related to the Adler Bell Jackiv anomaly [17]. It becomes clear that a relativistic treatment of the decay formula and of the normalization are important for a correct understanding of the pion as deeply bound quark antiquark state. This can also be seen in Fig.8 showing the upper and lower component Φ^{++} , Φ^{--} of the pion amplitude. In contrast to the wave function for the ρ meson (Fig.9) the upper pion amplitude is only about 10% larger than the lower one in the region of small relative momenta. For higher momenta the amplitudes even become equal. This fact obviously leads to important cancellations for the normalization and for the decay constant. This was already emphasized in an early quark model [18], where the effects of different estimates for the relation between the upper and lower component on weak decay constants for pion and kaon were analyzed. For a comparison with non-relativistic decay formulas compare Sec.IV D. Although the pion amplitude has significant contributions up to momenta of about 4GeV/c, the main part e.g. of the integral for the π^0 decay width comes from momenta of about 150 MeV/c (as this is the scale of nonstrange and pion mass).

For the $\eta \rightarrow \gamma\gamma$ decay we also find excellent agreement with experiment, whereas the process for the η' is underestimated. The results depend strongly on the correct $n\bar{n}$ - $s\bar{s}$ mixing, as e.g. for the η we obtain a negative interference. The mixing (due to the instanton induced interaction) can be compared to a simple model given by Rosner [19]. The physical mesons are expanded in a basis of three states $|N\rangle = 1/\sqrt{2}|u\bar{u} + d\bar{d}\rangle$, $|S\rangle = |s\bar{s}\rangle$ and $|G\rangle = |Gluonium\rangle$:

$$|\eta\rangle = X_\eta|N\rangle + Y_\eta|S\rangle + Z_\eta|G\rangle \quad (33)$$

The coefficients may be estimated from electromagnetic transitions [20]. We compared the results for the absolute values of X and Y in Tab.VI with the contributions of the nonstrange and strange part of the amplitude to the relativistic norm. The results agree well in the case of the η , but not for the η' . Experimental results indicate a larger gluonic component for the η' , which could modify the results.

The leptonic decay widths for the vector mesons are also in good agreement with the data. This is essentially due to the small confinement slope, which determines the size of these mesons. We conclude that a consistent description of all the ground state pseudoscalar and vector mesons is possible in this framework. However, more observables like electromagnetic transitions or the pion form factor will be calculated in the future to substantiate this statement.

The agreement with experimental data for model V2, which was designed to reproduce the higher resonances and Regge trajectories, is only of a qualitative character (Tab.V). Decay constants and photon decay widths disagree by about 50%, which is essentially due to the large

quark mass. The leptonic decay widths of the vector mesons are overestimated due to the steep confinement, which enlarges the amplitudes at the origin in coordinate space.

Comparing the two parameter sets for vector confinement we find: V1 with light quark masses gives a quantitative description for the vector and pseudoscalar ground states, but only a qualitative picture of the Regge behavior. For V2 with large quark masses the situation is opposite. This might be an indication that for large distances the mass of the quarks effectively should increase due to some additional mass of a string.

For model S we find good agreement for the vector mesons, but not as good for the pseudoscalars. Although it is possible to describe the latter with a smaller quark mass, we could not obtain a quantitative adjustment for both 0^- and 1^- with a scalar confining kernel.

D. Comparison with nonrelativistic results

In order to estimate the relevance of relativistic effects in our model it is useful to compare the results with the corresponding ones computed in the nonrelativistic quark model. In the nonrelativistic limit the Salpeter equation reduces to the usual Schrödinger equation with the hamiltonian given by

$$H = a_c + b_c r + 8 G_{f_2 f'_1, f_1 f'_2} \delta^3(\vec{r}) \quad (34)$$

where the δ -function again has to be regularized according to eq.(32). The mass spectra for this hamiltonian have already been investigated in an earlier work [2] being in good agreement with experiment. In the following we will use the wave functions $\psi(\vec{r})$ of [2] to calculate the decay observables using the well known formulas [14,21,22]

$$f_\pi = \frac{2\sqrt{3}}{\sqrt{M}} |\psi(0)| \quad (35)$$

$$\Gamma(1^- \rightarrow l^+ l^-) = \frac{16 \pi \alpha^2 \tilde{e}_q^2}{M^2} |\psi(0)|^2 \quad (36)$$

$$\Gamma(0^- \rightarrow \gamma\gamma) = \frac{12 \pi \alpha^2 \tilde{e}_q^4}{m_q^2} |\psi(0)|^2 \quad (37)$$

$$(38)$$

Here M is the experimental meson mass, m_q is the quark mass, $\alpha = 1/137$ and \tilde{e}_q gives the quark charge in units of the proton charge according to the flavor composition of the meson. The results for these decays are given in Tab.V. One finds that leptonic decays can already be described reasonably in a nonrelativistic framework. On the other hand the weak decay constants and especially the two photon decay widths are far away from the experimental data. This discrepancy cannot be cured by changing the parameters within reasonable limits. We therefore conclude that a relativistic treatment is essential for the pseudoscalar mesons.

E. Discussion of the gap equations

Due to the process of chiral symmetry breaking the 't Hooft interaction leads to relations for the effective constituent quark masses m_n , m_s and the coupling constants g , g' as given in eqs.(10). In order to check if these relations are qualitatively compatible with the fitted parameter sets we use $\Lambda_{QCD} = 200 \text{ MeV}$, $m_n^0 = 9 \text{ MeV}$, $m_s^0 = 150 \text{ MeV}$, $\langle \bar{q}_n q_n \rangle = (-225 \text{ MeV})^3$ and $\langle \bar{q}_s q_s \rangle = 0.8 \langle \bar{q}_n q_n \rangle$ (compare [23]) and plot m_n , m_s , g and g' as functions of the instanton size cutoff ρ_c as shown in Figs.6,7.

Because of the delicate dependence on the condensate values and due to the regularization procedure in the 't Hooft kernel one should not expect quantitative agreement with the fitted parameter sets.

For $\rho_c = 0.408 \text{ fm}$ one finds e.g. $m_n = 170 \text{ MeV}$, $m_s = 270 \text{ MeV}$, $g = 79 \text{ MeV fm}^3$ and $g' = 58 \text{ MeV fm}^3$. Despite of the strange quark mass which comes out too small the other parameters are quite close to the values of parameter set VI. Note that ρ_c is almost equal to the effective range Λ of the 't Hooft interaction. Furthermore we find that g' is smaller than g for all values of ρ_c as is the case for all three parameter sets.

V. SUMMARY AND CONCLUSION

Within the framework of the instantaneous Bethe Salpeter equation we investigated different models for mesons as bound states of quark and antiquark. We consider it to be the main result of this work that the masses, weak decay constants and two photon widths of the light pseudoscalar mesons (π , η , K) can be understood quantitatively in terms of a $q\bar{q}$ description, alternatively to the Goldstone picture. With the same parameters also the masses and leptonic decays of the vector mesons can be reproduced.

The pseudoscalar mesons are dominantly affected by an instanton induced interaction, which apart from the π, η splitting gives the correct $n\bar{n}$ –, $s\bar{s}$ –mixing for the η meson. The self energy corrections and coupling constants due to the resulting chiral symmetry breaking are compatible with the parameters we used for the quark antiquark interaction. In contrast to nonrelativistic calculations instanton effects appear also in the scalar sector and lead to a isoscalar state with imaginary mass and zero norm.

Concerning the nature of the confinement kernel we find that a vector type interaction can reproduce the Regge trajectories, although with a larger quark mass than the one needed to describe the lowest lying mesons. This might be an indication that due to string effects the quark mass should increase with distance.

We were only able to find reliable solutions with a scalar kernel for relatively large quark masses and weak

confinement. With these parameters, however, one cannot reproduce quantitatively the ground state mesons or the Regge trajectories. Nevertheless the spin orbit splitting indicates the existence of a scalar component in the interaction in order to cancel the large mass differences coming from the vector structure.

Acknowledgments: We are thankful to M.Fuchs for constant help in numerical questions.

APPENDIX A: THE 'T HOOFT INTERACTION

1. The Lagrangian

As shown by Shifman, Vainshtein and Zakharov [8] the contribution of an instanton-antiinstanton configuration to the effective quark Lagrangian for three quark flavors u , d , s is given by

$$\begin{aligned} \Delta \mathcal{L} = & \int d\rho \frac{d_0(\rho)}{\rho^5} \left\{ \left[\prod_{i=1}^3 \left(m_i^0 \rho - \frac{4}{3} \pi^2 \rho^3 (\bar{q}_i R q_{iL}) \right) \right. \right. \\ & + \frac{3}{32} \left(\frac{4}{3} \pi^2 \rho^3 \right)^2 \left[\left\{ (\bar{q}_{1R} \lambda^a q_{1L}) (\bar{q}_{2R} \lambda^a q_{2L}) \right. \right. \\ & - \frac{3}{4} (\bar{q}_{1R} \sigma_{\mu\nu} \lambda^a q_{1L}) (\bar{q}_{2R} \sigma^{\mu\nu} \lambda^a q_{2L}) \left. \right\} \\ & \left. \left(m_3^0 \rho - \frac{4}{3} \pi^2 \rho^3 (\bar{q}_{3R} q_{3L}) \right) \right. \\ & + \frac{9}{40} \left(\frac{4}{3} \pi^2 \rho^3 \right) d^{abc} (\bar{q}_{1R} \sigma_{\mu\nu} \lambda^a q_{1L}) \\ & \left. (\bar{q}_{2R} \sigma^{\mu\nu} \lambda^b q_{2L}) (\bar{q}_{3R} \lambda^c q_{3L}) \right. \\ & \left. + \text{cycl. perm. of (123)} \right] \\ & + \frac{9}{256} i \left(\frac{4}{3} \pi^2 \rho^3 \right)^3 f^{abc} (\bar{q}_{1R} \sigma_\mu^\nu \lambda^a q_{1L}) \\ & (\bar{q}_{2R} \sigma_\nu^\tau \lambda^b q_{2L}) (\bar{q}_{3R} \sigma_\tau^\mu \lambda^c q_{3L}) \\ & + \frac{9}{320} \left(\frac{4}{3} \pi^2 \rho^3 \right)^3 d^{abc} (\bar{q}_{1R} \lambda^a q_{1L}) (\bar{q}_{2R} \lambda^b q_{2L}) \\ & \left. (\bar{q}_{3R} \lambda^c q_{3L}) \right] + (R \leftrightarrow L) \left. \right\} \quad (\text{A1}) \end{aligned}$$

with $\sigma_{\mu\nu} := [\gamma_\mu, \gamma_\nu]/2$ and $q_{iL} := \frac{1}{2}(1 + \gamma_5)q_i$, $q_{iR} := \frac{1}{2}(1 - \gamma_5)q_i$ being the projections of the quark Dirac operators q_i onto left and right handed components. Furthermore $i = 1, 2, 3 = u, d, s$ denotes the flavor degrees of freedom, m_i^0 the corresponding current quark masses, λ^a ($a = 1, \dots, 8$) are the color matrices and f^{abc} , d^{abc} are the standard $SU(3)$ structure constants defined by the commutator $[\lambda^a, \lambda^b]_- = 2i f^{abc} \lambda^c$ and the anticommutator $[\lambda^a, \lambda^b]_+ = \frac{4}{3} \delta^{ab} + 2 d^{abc} \lambda^c$. The 't Hooft interaction leads to spontaneous chiral symmetry breaking as can be seen by normal ordering $\mathcal{L} = \mathcal{L}_0 + \Delta \mathcal{L}$

with respect to the physical QCD vacuum, where $\mathcal{L}_0 = \sum_{j=1}^3 (i\bar{q}_j \gamma^\mu \partial_\mu q_j - m_j^0 \bar{q} q)$ is the free quark Lagrangian. Using the Wick theorem one finally obtains eq.(9).

2. The interaction between two quarks

After normal ordering the two body interaction term is given by

$$\begin{aligned} \Delta\mathcal{L}(2) = g_{\text{eff}}(3) \left\{ : (\bar{q}_{1R} q_{1L} \bar{q}_{2R} q_{2L}) : \right. \\ \left. + \frac{3}{32} : \left[(\bar{q}_{1R} \lambda^a q_{1L}) (\bar{q}_{2R} \lambda^a q_{2L}) \right. \right. \\ \left. \left. - \frac{3}{4} (\bar{q}_{1R} \sigma_{\mu\nu} \lambda^a q_{1L}) (\bar{q}_{2R} \sigma^{\mu\nu} \lambda^a q_{2L}) \right] : \right. \\ \left. + (R \leftrightarrow L) \right\} + \text{cycl. perm. of (123)} \quad (\text{A2}) \end{aligned}$$

with $g_{\text{eff}}(i)$ given in eq.(14). One can transform the two body force into a more transparent form using the notation ε_{ijk} , $i = u, d, s$ with $\varepsilon_{uds} = 1$. Insert $q_{iL,R} = (1 \pm \gamma_5)/2 q_i$ and use the relations

$$\sigma_{\mu\nu} \cdot \sigma^{\mu\nu} + \sigma_{\mu\nu} \gamma_5 \cdot \sigma^{\mu\nu} \gamma_5 = -4 (\Sigma^i \cdot \Sigma^i + \gamma_5 \Sigma^i \cdot \gamma_5 \Sigma^i) \quad (\text{A3})$$

with $\Sigma = \text{diag}(\sigma, \sigma)$ where the notation $(A \cdot B)_{ij,kl} = A_{ik} B_{jl}$ has been used. Furthermore use

$$\begin{aligned} \Sigma^k \cdot \Sigma^k &= 2 \Pi^S - 1^S \\ \lambda^a \cdot \lambda^a &= 2 \Pi^C - \frac{2}{3} 1^C \end{aligned} \quad (\text{A4})$$

with Π^S , Π^F and Π^C being exchange operators in spin, flavor and color defined as $\Pi_{ij,kl} = \delta_{il} \delta_{jk}$. On the anti-symmetric tensors one has $\Pi^S \Pi^F \Pi^C = -1$ which can be used to eliminate the spin dependence leading to eq.(13).

APPENDIX B: NUMERICAL SOLUTION OF THE SALPETER EQUATION

1. General framework

In this section we briefly sketch the numerical method outlined in ref. [1]. With the standard Dirac representation (see e.g. [24]) Φ is a 4×4 -matrix in spinor space that can be written in block matrix form as

$$\Phi = \begin{pmatrix} \Phi^{+-} & \Phi^{++} \\ \Phi^{--} & \Phi^{-+} \end{pmatrix} = \hat{\Phi} (\Phi^{++}, \Phi^{--}) \quad (\text{B1})$$

where each component is a 2×2 -matrix. The definition of the bilinear function $\hat{\Phi}$ is motivated by the fact that only two of these four amplitudes are independent since the Salpeter equation implies

$$\begin{aligned} \Phi^{+-} &= +c_1 \Phi^{++s} - c_2 s \Phi^{--} \\ \Phi^{-+} &= -c_1 \Phi^{--s} + c_2 s \Phi^{++} \end{aligned} \quad (\text{B2})$$

where we use the shorthand notation $s = \vec{\sigma} \vec{p}$, $c_i = \omega_i / (\omega_1 m_2 + \omega_2 m_1)$.

The transformation properties of the Salpeter amplitude imply that we can decompose Φ^{++} , Φ^{--} as

$$\begin{aligned} \Phi^{++}(\vec{p}) &= \sum_{LS} \mathcal{R}_{LS}^{(+)}(p) [Y_L(\Omega_p) \otimes \varphi_S]^J \\ \Phi^{--}(\vec{p}) &= \sum_{LS} \mathcal{R}_{LS}^{(-)}(p) [Y_L(\Omega_p) \otimes \varphi_S]^J \end{aligned} \quad (\text{B3})$$

with the spin matrix $(\varphi_{Sq} i\sigma_2)_{mm'} = \langle 1/2 m \ 1/2 m' | S q \rangle$. L , S have to respect the usual constraints coming from parity and charge conjugation. Let

$$E_i(\vec{p}) = R_{n_i L_i}(p) [Y_{L_i}(\Omega_p) \otimes \varphi_{S_i}]_{M_i}^J \quad (\text{B4})$$

be a complete set of 2×2 basis functions orthonormal with respect to the scalar product given by $(E_i | E_j) = \int \text{tr} [E_i^\dagger(\vec{p}) E_j(\vec{p})] = \delta_{ij}$. These basis functions can be used to expand Φ^{++} and Φ^{--} with corresponding (usually real) expansion coefficients $a_i^{(+)}$ and $a_i^{(-)}$. Inserting these expansions into $\hat{\Phi}$ gives

$$\psi = \sum_{i=1}^{\infty} \left(a_i^{(+)} e_i^{(+)} + a_i^{(-)} e_i^{(-)} \right) \quad (\text{B5})$$

with $e_i^{(+)} = \hat{\Phi}(E_i, 0) \gamma^0$ and $e_i^{(-)} = \hat{\Phi}(0, E_i) \gamma^0$. Defining the matrix elements (which are real in our case) $H_{ij}^{ss'} = \langle e_i^{(s)} | \mathcal{H} e_j^{(s')} \rangle$ and $N_{ij}^{ss'} = \langle e_i^{(s)} | e_j^{(s')} \rangle$ the Salpeter equation $\mathcal{H}\psi = M\psi$ can now be written in the form of a matrix equation as

$$\begin{pmatrix} H^{++} & H^{+-} \\ H^{+-} & H^{--} \end{pmatrix} \begin{pmatrix} a^{(+)} \\ a^{(-)} \end{pmatrix} = M \begin{pmatrix} N^{++} & 0 \\ 0 & -N^{++} \end{pmatrix} \begin{pmatrix} a^{(+)} \\ a^{(-)} \end{pmatrix} \quad (\text{B6})$$

We solve this equation within a finite basis $i \leq i_{max} = 10$ and use the variational principle $\delta M = 0$ looking for stationary points of M as a function of β , where β is a variational parameter with the physical dimension MeV^{-1} that sets the absolute scale of the basis functions as $E_i^\beta(\vec{p}) = \beta^{3/2} E_i^{\beta=1}(\vec{p}\beta)$. For the basis functions in momentum space the following functions have been used:

$$R_{nL}(y) = N_{nL} y^L L_n^{2L+2}(y) e^{-y/2} \quad (\text{B7})$$

with N_{nL} being a normalization coefficient, $y = p\beta$ and $L_n^{2L+2}(y)$ being a Laguerre polynomial. The fouriertransformed basis states also can be given in analytical form. About ten basis states are sufficient to solve the Salpeter equation with rather high accuracy. The usual choice of 3-dimensional harmonic oscillator functions is less favored here since their asymptotic behavior $\sim e^{-y^2/2}$ for $y \rightarrow \infty$ turns out to be not appropriate for deeply bound states like the pion. For other mesons, however, we have checked that both basis systems give equal results within numerical errors.

2. Expectation values

In order to compute the matrix elements present in eq.(B6) it is useful to rewrite $\langle\psi|\psi\rangle$ and $\langle\psi|\mathcal{H}\psi\rangle$ in terms of Φ^{++} and Φ^{--} using eq.(B2). We find

$$\langle\psi|\psi\rangle = \frac{2\omega_1\omega_2}{\omega_1 m_2 + \omega_2 m_1} \text{tr}((\Phi^{++})^\dagger \Phi^{++} - (\Phi^{--})^\dagger \Phi^{--}) \quad (\text{B8})$$

for the norm. The matrix elements of \mathcal{H} can be split as

$$\langle\psi|\mathcal{H}\psi\rangle = \langle\psi|\mathcal{T}\psi\rangle + \langle\psi|\mathcal{V}\psi\rangle \quad (\text{B9})$$

$$\langle\psi|\mathcal{T}\psi\rangle = \int (\omega_1 + \omega_2) \text{tr}[\Phi^\dagger \Phi] \quad (\text{B10})$$

$$\langle\psi|\mathcal{V}\psi\rangle = - \int \int' \text{tr}[\Phi^\dagger \gamma^0 (V\Phi') \gamma^0] \quad (\text{B11})$$

with $\int = \int d^3p/(2\pi)^3$. The basic formula for the calculation of the kinetic energy and confinement matrix elements is given by

$$\begin{aligned} \text{tr}(\Phi^\dagger \Phi') &= \quad (\text{B12}) \\ &= \text{tr}[(\Phi^{++})^\dagger (\Phi^{++})' + (\Phi^{--})^\dagger (\Phi^{--})' + \\ &\quad + (\Phi^{+-})^\dagger (\Phi^{+-})' + (\Phi^{-+})^\dagger (\Phi^{-+})'] = \\ &= \text{tr}[(\Phi^{++})^\dagger (\Phi^{++})' + (\Phi^{--})^\dagger (\Phi^{--})' + \\ &\quad + c_1 c_1' (\Phi^{++})^\dagger (\Phi^{++})' s' s - c_1 c_2' (\Phi^{++})^\dagger s' (\Phi^{--})' s - \\ &\quad - c_2 c_1' (\Phi^{--})^\dagger s (\Phi^{++})' s' + c_2 c_2' (\Phi^{--})^\dagger s s' (\Phi^{--})' + \\ &\quad + c_1 c_1' (\Phi^{--})^\dagger (\Phi^{--})' s' s - c_1 c_2' (\Phi^{--})^\dagger s' (\Phi^{++})' s - \\ &\quad - c_2 c_1' (\Phi^{++})^\dagger s (\Phi^{--})' s' + c_2 c_2' (\Phi^{++})^\dagger s s' (\Phi^{++})'] \end{aligned}$$

where the prime indicates the dependence on \vec{p}' . To compute the kinetic energy term eq.(B10) set $\vec{p}' = \vec{p}$ in this equation.

For the interaction term eq.(B11) we investigate the following contributions:

a. Scalar confinement

From the scalar confining kernel eq.(8) one has

$$\langle\psi|\mathcal{V}_C^S\psi\rangle = - \int \int' \mathcal{V}_C \text{tr}[\Phi^\dagger \gamma^0 \Phi' \gamma^0] \quad (\text{B13})$$

with $\mathcal{V}_C = \mathcal{V}_C((\vec{p} - \vec{p}')^2)$. Since

$$\gamma^0 \Phi \gamma^0 = \begin{pmatrix} \Phi^{+-} & -\Phi^{++} \\ -\Phi^{--} & \Phi^{-+} \end{pmatrix} \quad (\text{B14})$$

the expression for $\text{tr}[\Phi^\dagger \gamma^0 \Phi' \gamma^0]$ is obtained by changing the sign of the first two terms $(\Phi^{++})^\dagger (\Phi^{++})'$ and $(\Phi^{--})^\dagger (\Phi^{--})'$ in eq.(B12).

b. Vector confinement

From the vector confining kernel eq.(7) one has

$$\langle\psi|\mathcal{V}_C^V\psi\rangle = \int \int' \mathcal{V}_C \text{tr}[\Phi^\dagger \Phi'] \quad (\text{B15})$$

and eq.(B12) can be applied directly. Note that a covariant form to write the vector confinement kernel is

$$\begin{aligned} [K(P, p, p') \chi(p')] &= \quad (\text{B16}) \\ &= -\mathcal{V}_C((p_\perp - p'_\perp)^2) \frac{1}{P^2} P^\mu \gamma_\mu \chi(p') P^\nu \gamma_\nu \end{aligned}$$

with $p_\perp = p - (Pp)/P^2$, so that the relation

$$P^\mu \frac{d}{dP^\mu} [K(P, p, p')] = 0 \quad (\text{B17})$$

holds as is required to rewrite the normalization condition for Φ .

c. 't Hooft interaction

From the 't Hooft kernel eq.(30) we find (omitting flavor indices)

$$\begin{aligned} \langle\psi|\mathcal{V}_T\psi\rangle &= \quad (\text{B18}) \\ &= -4G \int \int' \text{tr}[\Phi^\dagger \gamma^0 (1_4 \text{tr} \Phi' + \gamma^5 \text{tr}(\Phi' \gamma^5)) \gamma^0] = \\ &= -4G \int \int' [(\text{tr} \Phi)^* (\text{tr} \Phi') - (\text{tr} \Phi \gamma^5)^* (\text{tr} \Phi' \gamma^5)] \end{aligned}$$

with

$$\begin{aligned} \text{tr} \Phi &= \text{tr}(\Phi^{+-} + \Phi^{-+}) \\ \text{tr}(\Phi \gamma^5) &= \text{tr}(\Phi^{++} + \Phi^{--}) \end{aligned} \quad (\text{B19})$$

Using the decomposition eq.(B3) and $\text{tr} \varphi_{S_q} = \sqrt{2} \delta_{S_0}$ one obtains

$$\text{tr} \Phi_{JM_J}^{++}(\vec{p}) = \sqrt{2} \mathcal{R}_{NJ_0}^{(+)}(p) Y_{JM_J}(\Omega_p) \delta_{S_0} \quad (\text{B20})$$

$$\text{tr} \Phi_{JM_J}^{--}(\vec{p}) = \sqrt{2} \mathcal{R}_{NJ_0}^{(-)}(p) Y_{JM_J}(\Omega_p) \delta_{S_0} \quad (\text{B21})$$

We further see that

$$\text{tr}(\varphi_{S_q} \vec{\sigma} \vec{p}) = \text{tr}(\vec{\sigma} \vec{p} \varphi_{S_q}) = \sqrt{2} \delta_{S_1} p_q \quad (\text{B22})$$

with the spherical components $p_q = \sqrt{4\pi/3} p Y_{1q}(\Omega_p)$. We find

$$\int d\Omega_p \text{tr}(\Phi \gamma^5) = \quad (\text{B23})$$

$$= \sqrt{2} \sqrt{4\pi} (\mathcal{R}_{NJ_0}^{(+)}(p) + \mathcal{R}_{NJ_0}^{(-)}(p)) \delta_{S_0} \delta_{L_0} \delta_{J_0}$$

$$\int d\Omega_p \text{tr} \Phi = \quad (\text{B24})$$

$$= -\sqrt{2} \sqrt{4\pi} p (c_1 + c_2) (\mathcal{R}_{NJ_0}^{(+)}(p) - \mathcal{R}_{NJ_0}^{(-)}(p)) \delta_{S_1} \delta_{L_1} \delta_{J_0}$$

3. Matrix elements

The expressions obtained above can now be used to compute the required matrix elements. In order to calculate e.g. $N_{ij}^{++} = \langle e_i^{(+)} | e_j^{(+)} \rangle$ one has to replace in eq.(B8) $(\Phi^{++})^\dagger$ by E_i^\dagger and Φ^{++} by E_j setting $(\Phi^{--})^\dagger = 0$ and $\Phi^{--} = 0$. In the following we will use the notation

$$(i|f(p)|j) = \int \frac{p^2 dp}{(2\pi)^3} R_{n_i L_i}(p) R_{n_j L_j}(p) f(p) \quad (\text{B25})$$

for the radial integrals between the basis states. These integrals can be effectively computed numerically using e.g. Gauss quadrature routines. According to eq.(B9) we write $H_{ij}^{ss'} = T_{ij}^{ss'} + V_{ij}^{ss'}$ with $V_{ij}^{ss'} = (V_C)_{ij}^{ss'} + (V_T)_{ij}^{ss'}$.

a. Normalization matrix elements

For the normalization matrix elements we find from eq.(B8)

$$N_{ij}^{++} = -N_{ij}^{--} = \left(i \left| \frac{2\omega_1\omega_2}{\omega_1 m_2 + \omega_2 m_1} \right| j \right) \quad (\text{B26})$$

$$N_{ij}^{+-} = N_{ij}^{-+} = 0 \quad (\text{B27})$$

b. Kinetic energy matrix elements

In order to evaluate the angular momentum structure of matrix elements the relation $(-i\sigma_2) \vec{\sigma} (i\sigma_2) = -^t \vec{\sigma}$ is quite useful. Define the $q\bar{q}$ spin matrix as $\chi_{S_q} = \varphi_{S_q} i\sigma_2$ and use $s = \vec{\sigma}\vec{p}$. Then one can write e.g.

$$\begin{aligned} & \text{tr}(\varphi_{S_i M_i}^\dagger s \varphi_{S_j M_j} s) \\ &= -\text{tr}(\chi_{S_i M_i}^\dagger (s_1 \otimes s_2) \chi_{S_j M_j}) = \\ &=: -\langle S_i M_i | s_1 \otimes s_2 | S_j M_j \rangle \end{aligned} \quad (\text{B28})$$

with $s_i = 2\vec{S}_i \vec{p}$ where \vec{S}_1 is the spin operator acting on the first quark and \vec{S}_2 on the second quark. It is useful to define

$$\begin{aligned} S_1(L', S', L, S, J) &:= \langle [L' \otimes S']^J | s_1/p | [L \otimes S]^J \rangle \\ S_2(L', S', L, S, J) &:= \langle [L' \otimes S']^J | s_2/p | [L \otimes S]^J \rangle \\ S_{12}(L', S', L, S, J) &:= \langle [L' \otimes S']^J | (s_1 \otimes s_2)/p^2 | [L \otimes S]^J \rangle \end{aligned} \quad (\text{B29})$$

Using the Wigner-Eckart theorem and the notation $\hat{L} = \sqrt{2L+1}$ one has

$$\begin{aligned} S_1(L', S', L, S, J) &= (-1)^{S+S'} S_2(L', S', L, S, J) = \\ &= (-1)^{L'+1} \hat{J} \hat{L}' \hat{L} \hat{S}' \hat{S} \sqrt{9} \sqrt{12} \begin{pmatrix} L' & 1 & L \\ 0 & 0 & 0 \end{pmatrix} \\ &\cdot \begin{Bmatrix} L' & S' & J \\ L & S & J \\ 1 & 1 & 0 \end{Bmatrix} \begin{pmatrix} 1/2 & 1/2 & S' \\ 1/2 & 1/2 & S \\ 1 & 0 & 1 \end{pmatrix} \end{aligned} \quad (\text{B30})$$

$$\begin{aligned} S_{12}(L', S', L, S, J) &= \\ &= \sum_{L_k S_k} S_1(L', S', L_k, S_k, J) S_2(L_k, S_k, L, S, J) \end{aligned} \quad (\text{B31})$$

The kinetic energy matrix elements are now given by

$$\begin{aligned} T_{ij}^{++} &= T_{ij}^{--} = \\ &= (i | (\omega_1 + \omega_2) (1 + p^2 (c_1^2 + c_2^2)) | j) \delta_{L_i L_j} \delta_{S_i S_j} \\ T_{ij}^{+-} &= T_{ij}^{-+} = \\ &= (i | (\omega_1 + \omega_2) 2 p^2 c_1 c_2 | j) S_{12}(i, j) \end{aligned} \quad (\text{B32})$$

with $S_{12}(i, j) = S_{12}(L_i, S_i, L_j, S_j, J)$.

c. Scalar and vector confinement matrix elements

The confinement matrix elements can be computed by inserting two complete sets of basis functions like

$$\begin{aligned} \langle i | f_1(\vec{p}) V(r) f_2(\vec{p}') | j \rangle &= \\ &= \sum_{g,h} \langle i | f_1(\vec{p}) | g \rangle \langle g | V(r) | h \rangle \langle h | f_2(\vec{p}') | j \rangle \end{aligned} \quad (\text{B33})$$

where the matrix element of V can be evaluated in coordinate space. One finds for the scalar confinement matrix elements

$$\begin{aligned} (V_C^S)_{ij}^{++} &= (V_C^S)_{ij}^{--} = (i | \mathcal{V}_C | j) - \sum_{g,h} \\ &\left\{ (i | p c_1 | g) S_2(i, g) (g | \mathcal{V}_C | h) (h | p c_1 | j) S_2(h, j) \right. \\ &\left. + (i | p c_2 | g) S_1(i, g) (g | \mathcal{V}_C | h) (h | p c_2 | j) S_1(h, j) \right\} \end{aligned} \quad (\text{B34})$$

and

$$\begin{aligned} (V_C^S)_{ij}^{+-} &= (V_C^S)_{ij}^{-+} = - \sum_{g,h} \\ &\left\{ (i | p c_1 | g) S_2(i, g) (g | \mathcal{V}_C | h) (h | p c_2 | j) S_1(h, j) \right. \\ &\left. + (i | p c_2 | g) S_1(i, g) (g | \mathcal{V}_C | h) (h | p c_1 | j) S_2(h, j) \right\} \end{aligned} \quad (\text{B35})$$

with

$(g | \mathcal{V}_C | h) = \int r^2 dr R_{n_i L_i}^F(r) R_{n_j L_j}^F(r) \mathcal{V}_C^F(r) \delta_{L_i L_j} \delta_{S_i S_j}$ where R^F denotes the Fourier transformed basis functions and $\mathcal{V}_C^F(r) = a_c + b_c r$.

For the vector confinement matrix elements one only has to change the sign of $\sum_{g,h}$ in the two equations above.

d. 't Hooft matrix elements

The 't Hooft matrix elements with the regularizing potential can be computed analogously to the confinement

matrix elements. In the unregularized case $\Lambda \rightarrow 0$ corresponding to $\mathcal{V}_{\text{reg}}^F(r) \rightarrow \delta(\vec{r})$ only $L = 0$ basis states contribute to $(g|\mathcal{V}_{\text{reg}}|h)$. Consistently only $L = 0$ states will be taken into account for $(g|\mathcal{V}_{\text{reg}}|h)$ also for $\Lambda > 0$ so that the angular selection rules are not changed by the regularization. The result for $L = S = 0$ reads

$$\begin{aligned} (V_T^{++})_{ij}^{S=0} &= (V_T^{--})_{ij}^{S=0} = (V_T^{+-})_{ij}^{S=0} = (V_T^{-+})_{ij}^{S=0} \\ &= 8G (i|\mathcal{V}_{\text{reg}}|j) \delta_{S_i 0} \delta_{S_j 0} \delta_{L_i 0} \delta_{L_j 0} \delta_{J 0} \end{aligned} \quad (\text{B36})$$

and for $L = S = 1$

$$\begin{aligned} (V_T^{++})_{ij}^{S=1} &= (V_T^{--})_{ij}^{S=1} = -(V_T^{+-})_{ij}^{S=1} = -(V_T^{-+})_{ij}^{S=1} \\ &= -8G \sum_{g,h} (i|p(c_1 + c_2)|g) (g|\mathcal{V}_{\text{reg}}|h) (h|p(c_1 + c_2)|j) \\ &\quad \delta_{S_i 1} \delta_{S_j 1} \delta_{L_i 1} \delta_{L_j 1} \delta_{J 0} \end{aligned} \quad (\text{B37})$$

This result shows that the 't Hooft interactions affects only mesons with $J = 0$ and $L = S = 0$ (i.e. pseudoscalar mesons with $J^{\pi P} = 0^-$) or $L = S = 1$ (i.e. scalar mesons with $J^{\pi P} = 0^+$). In the nonrelativistic limit the contributions to the scalar mesons vanish.

-
- [1] J.Resag, C.R.Münz, B.C.Metsch, H.R.Petry: Analysis of the instantaneous Bethe-Salpeter equation for $q\bar{q}$ -bound-states
 - [2] W.H.Blask, U.Bohn, M.G.Huber, B.C.Metsch, H.R.Petry: Z.Phys.A 337, 327 (1990)
 - [3] Y.Nambu, G.Jona-Lasinio: Phys.Rev. 122, 345 (1961)
 - [4] S.Klimt et.al., Nucl.Phys. A516, 429 (1990)
 - [5] Progress in particle and nuclear physics, Vol.27, editor: A.Faessler, pergamon press 1991, chapter 4 by U.Vogl, W.Weise, 195
 - [6] J.F.Lagaë: Phys.Rev. D45, 305, 317 (1992)
 - [7] G.'t Hooft: Phys.Rev. D14, 3432 (1976)
 - [8] M.A.Shifman, A.I.Vainshtein, V.I.Zakharov: Nucl.Phys. B163, 46 (1980)
 - [9] H.R.Petry et.al., Phys.Lett 159B, 363 (1985)
 - [10] W.Lucha, F.F.Schöberl, D.Gromes: Phys.Rep. 200, No.4, 127 (1991)
 - [11] D.Gromes: Z.Phys.C-Particles and Fields 26, 401 (1984)
 - [12] S.N.Biwas, S.R.Choudhury, K.Datta, A.Goyal: Phys.Rev. D26, 1983 (1982)
 - [13] A.Gara, B.Durand, L.Durand, L.J.Nickisch: Phys.Rev. D40, 843 (1989)
A.Gara, B.Durand, L.Durand: Phys.Rev. D42, 1651 (1990)
 - [14] M.Beyer, U.Bohn, M.G.Huber, B.C.Metsch, J.Resag: Z.Phys.C-Particles and Fields 55, 307 (1992)
 - [15] E.V.Shuryak: Nucl.Phys. B203, 93 (1982)
 - [16] B.Silvestre-Brac, C.Gignoux: Preprint, Institut des Sciences Nucléaires, Grenoble 1989
 - [17] S.L.Adler: Phys.Rev. 177,2426 (1969)
J.S.Bell,R.Jackiv: Nuovo Cimento 60A, 47 (1969)

- [18] C.H. Llewellyn Smith, Ann.Phys. 53, 521 (1969)
Phys.Rep. 200, No.4, 127 (1991)
- [19] J.L.Rosner, Phys.Rev. D27 1101 (1983)
- [20] R.M.Baltrusaitis et al.: Phys.Rev. D32, 2883 (1985)
- [21] R.van Royen, V.F.Weisskopf: Nuov.Cim. 50,2 A, 617 (1967)
- [22] W.Kwong, J.L.Rosner, C.Quigg: Ann.Rev.Nucl.Part.Sci. 37, 325 (1987)
- [23] L.J.Reinders, H.Rubinstein, S.Yazaki: Phys.Rep.Vol.127, 1 (1985)
- [24] C.Itzykson, J.-B.Zuber: Quantum Field Theory, New York: McGraw-Hill 1985
- [25] Particle Data Group, Phys.Rev. D45 Part II (1992)

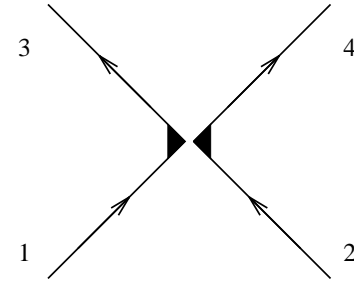


FIG. 1. Instanton induced interaction vertex corresponding to $\Delta\mathcal{L}_2$.

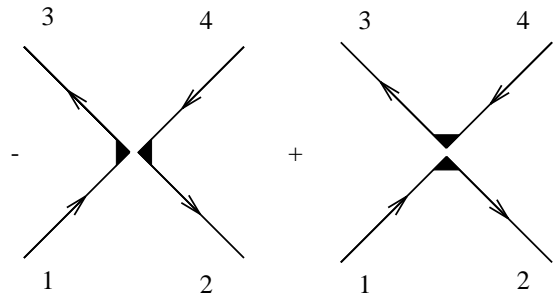


FIG. 2. Instanton induced interaction vertices for $q\bar{q} \rightarrow q\bar{q}$.

FIG. 3. Mass spectra of the pseudoscalar mesons. The columns for each meson correspond (from the left) to model V1, model V2, experiment [25] and model S. The shaded areas (3rd column) indicate the experimental full width of the meson.

FIG. 4. Mass spectra of the vector mesons (see also caption to Fig. 3).

FIG. 5. Regge trajectory for the isovector mesons with $S = 1$. The solid line shows the experimental masses for ρ , a_2 , ρ_3 , a_4 [25] where the errorbar gives the experimental error for the resonance position. The short dashed line corresponds to the calculated masses of model V1, the dotted line to model V2 and the long dashed line to the scalar confinement (model S).

FIG. 6. Effective mass dependence for the non strange (solid curve) and strange quark (dashed curve) on the instanton size cutoff ρ_c .

FIG. 7. Effective coupling constants for the instanton induced non-strange quark interaction g (solid curve) and the strange non-strange quark interaction g' (dashed curve) as a function of the instanton size cutoff ρ_c , see eq.(14,26)

FIG. 8. Radial Pion amplitudes $p\mathcal{R}_{00}^{(+)}(p)$ (upper component, solid curve) and $p\mathcal{R}_{00}^{(-)}(p)$ (lower component, dashed curve) with the parameters of model V1

FIG. 9. Radial Rho amplitudes $p\mathcal{R}_{01}^{(+)}(p)$ (upper s-wave component, solid curve), $p\mathcal{R}_{01}^{(-)}(p)$ (lower s-wave component, long dashed curve), $p\mathcal{R}_{21}^{(+)}(p)$ (upper d-wave component, dashed dotted curve), $p\mathcal{R}_{21}^{(-)}(p)$ (lower d-wave component, short dashed curve) with the parameters of model V1

TABLE I. Flavor dependence of the instanton induced interaction $G_{f_2 f_3, f_1 f_4}$ (see eq.(22))

$f_1 f_2 \rightarrow$	$u\bar{d}$	$d\bar{u}$	$u\bar{s}$	$d\bar{s}$	$s\bar{d}$	$s\bar{u}$	$u\bar{u}$	$d\bar{d}$	$s\bar{s}$
$f_3 f_4 \downarrow$									
$u\bar{d}$	-g	0							
$d\bar{u}$	0	-g							
$u\bar{s}$			-g'	0	0	0			
$d\bar{s}$			0	-g'	0	0			
$s\bar{d}$			0	0	-g'	0			
$s\bar{u}$			0	0	0	-g'			
$u\bar{u}$							0	g	g'
$d\bar{d}$							g	0	g'
$s\bar{s}$							g'	g'	0

TABLE II. Flavor matrix elements of $G_{f_2 f_3, f_1 f_4}$ for pseudoscalar mesons

	π^0	η_n	η_s
π^0	-g	0	0
η_n	0	g	$\sqrt{2}g'$
η_s	0	$\sqrt{2}g'$	0

TABLE III. Parameters of the different models (see Sec.IV A)

Parameter	V1	V2	S
m_n [MeV]	170	340	340
m_s [MeV]	390	568	487
a_c [MeV]	-552	-1340	-998
b_c [MeV/fm]	570	1400	1000
g [MeV fm ³]	51.67	34.65	44.79
g' [MeV fm ³]	46.92	30.84	41.01
Λ [fm]	0.42	0.42	0.42

TABLE IV. Spin orbit splitting for the first positive parity mesons and the effect of the instanton induced interaction on the 0^{++} mesons, where a * denotes the existence of an additional state with imaginary mass and zero norm, see Sec.IV B (all Masses in MeV).

Meson	J^{PC} I	V1	V2	S
$a_0(980)$	$0^{++} 1$	960	1130	1260
$f_0(975)$	$0^{++} 0$	950*	1270*	950
$f_1(1285)$	$1^{++} 0$	930	1060	1150
$f_2(1270)$	$2^{++} 0$	1100	1280	1010

TABLE V. Comparison of experimental and calculated meson decay observables for the Salpeter models V1, V2, S and nonrelativistic results NR

Mesonic decay	experimental [25]	V1	V2	S	NR
f_π [MeV]	131.7 ± 0.2	130	260	200	1440
f_K [MeV]	160.6 ± 1.4	180	300	210	730
$\Gamma(\pi^0 \rightarrow \gamma\gamma)$ [eV]	7.8 ± 0.5	7.6	4.0	4.4	30000
$\Gamma(\eta \rightarrow \gamma\gamma)$ [eV]	460 ± 5	440	220	220	18500
$\Gamma(\eta' \rightarrow \gamma\gamma)$ [eV]	4510 ± 260	2900	2030	1390	750
$\Gamma(\rho \rightarrow e^+e^-)$ [keV]	6.8 ± 0.3	6.8	28	8.1	8.95
$\Gamma(\omega \rightarrow e^+e^-)$ [keV]	0.60 ± 0.02	0.73	3.1	0.87	0.96
$\Gamma(\phi \rightarrow e^+e^-)$ [keV]	1.37 ± 0.05	1.24	4.5	1.50	2.06

TABLE VI. η, η' mixing parameters from BS norm (see eq.(5)) compared to data calculated from experimental J/Ψ decays [20]

Meson	mixing coefficient	J/Ψ decay	V1	V2	S
$\eta(547)$	$ X_\eta $	0.63 ± 0.06	0.71	0.71	0.70
	$ Y_\eta $	0.83 ± 0.13	0.70	0.70	0.72
$\eta'(958)$	$ X_{\eta'} $	0.36 ± 0.05	0.85	0.78	0.83
	$ Y_{\eta'} $	0.72 ± 0.12	0.52	0.63	0.55

Fig.3

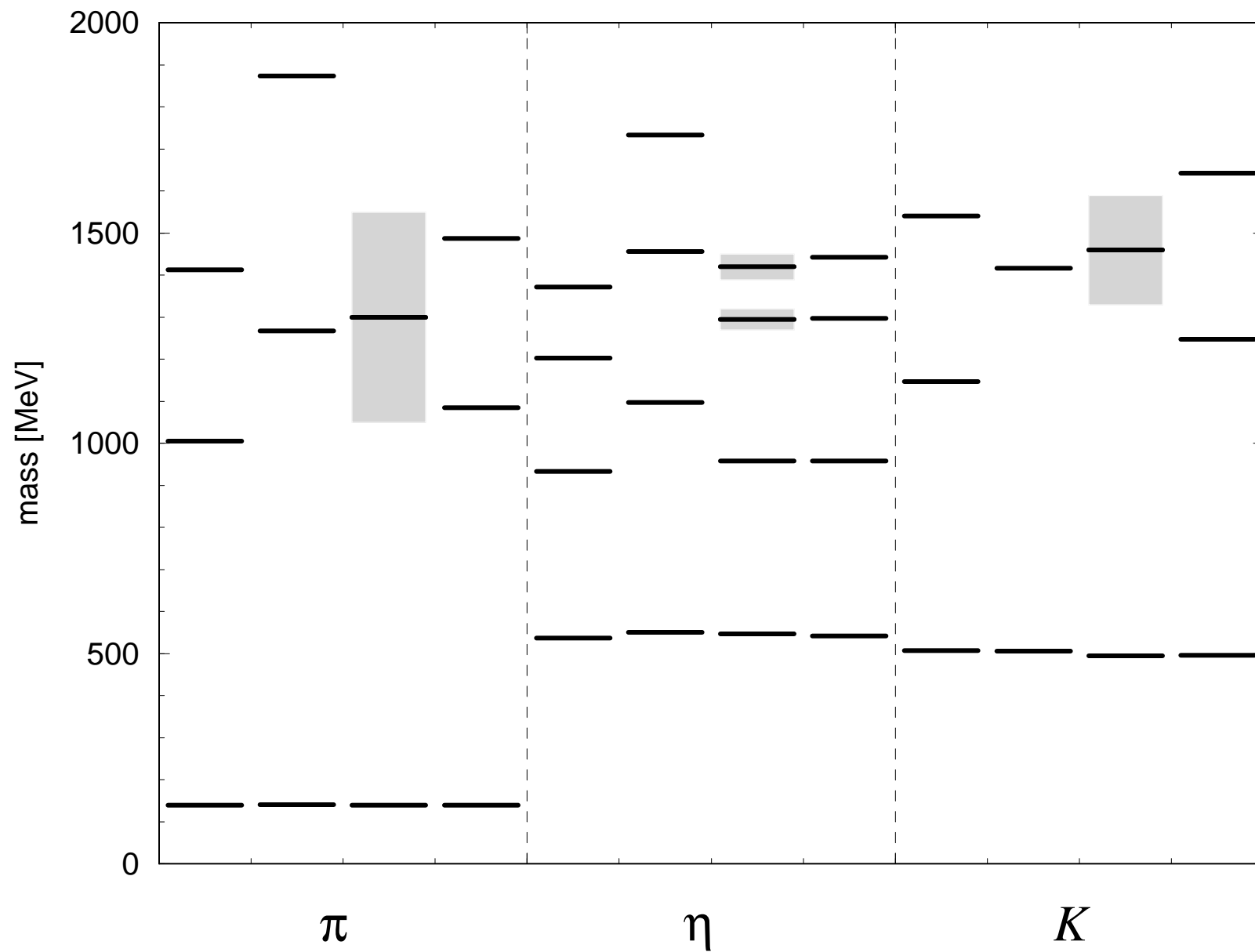


Fig.4

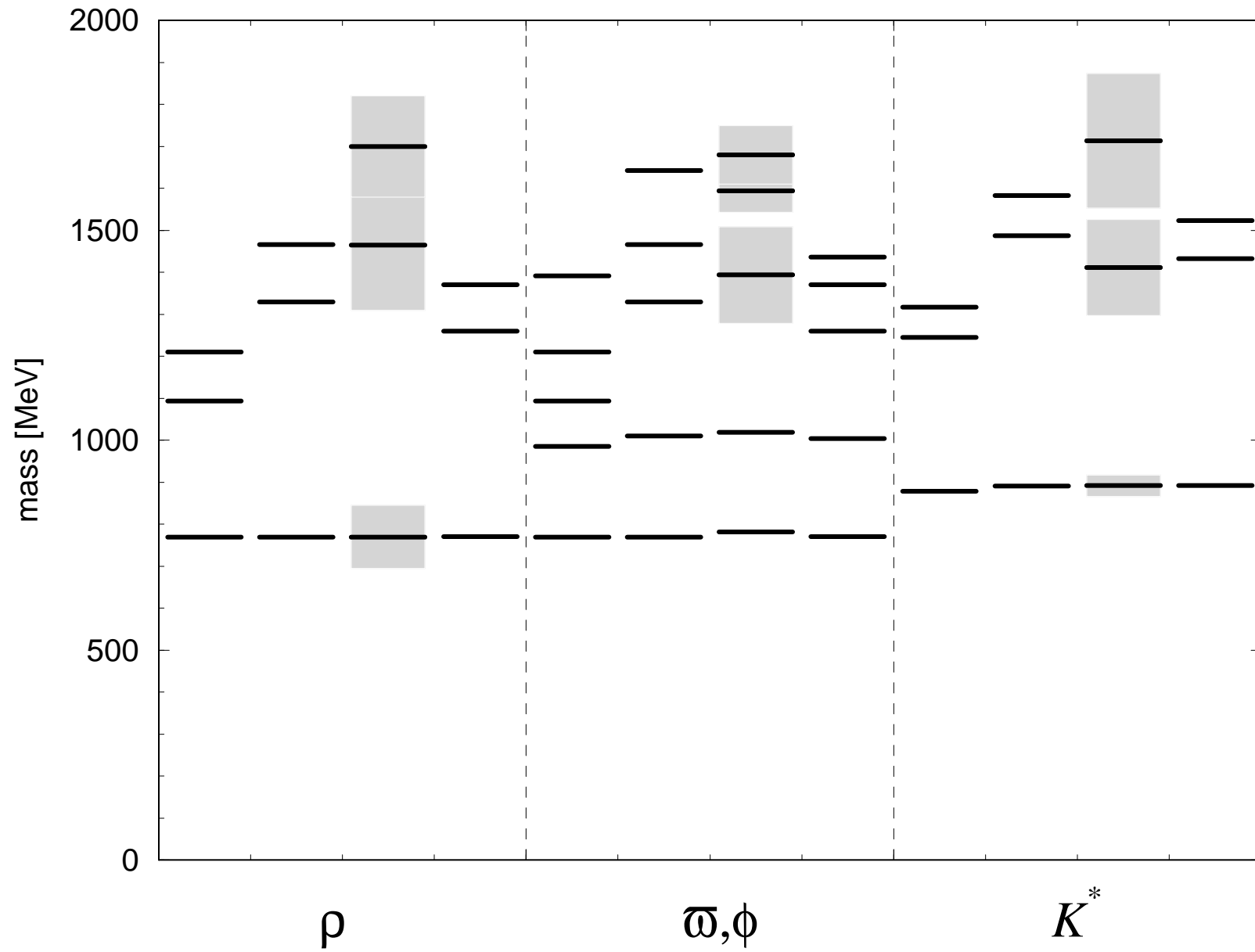


Fig.5

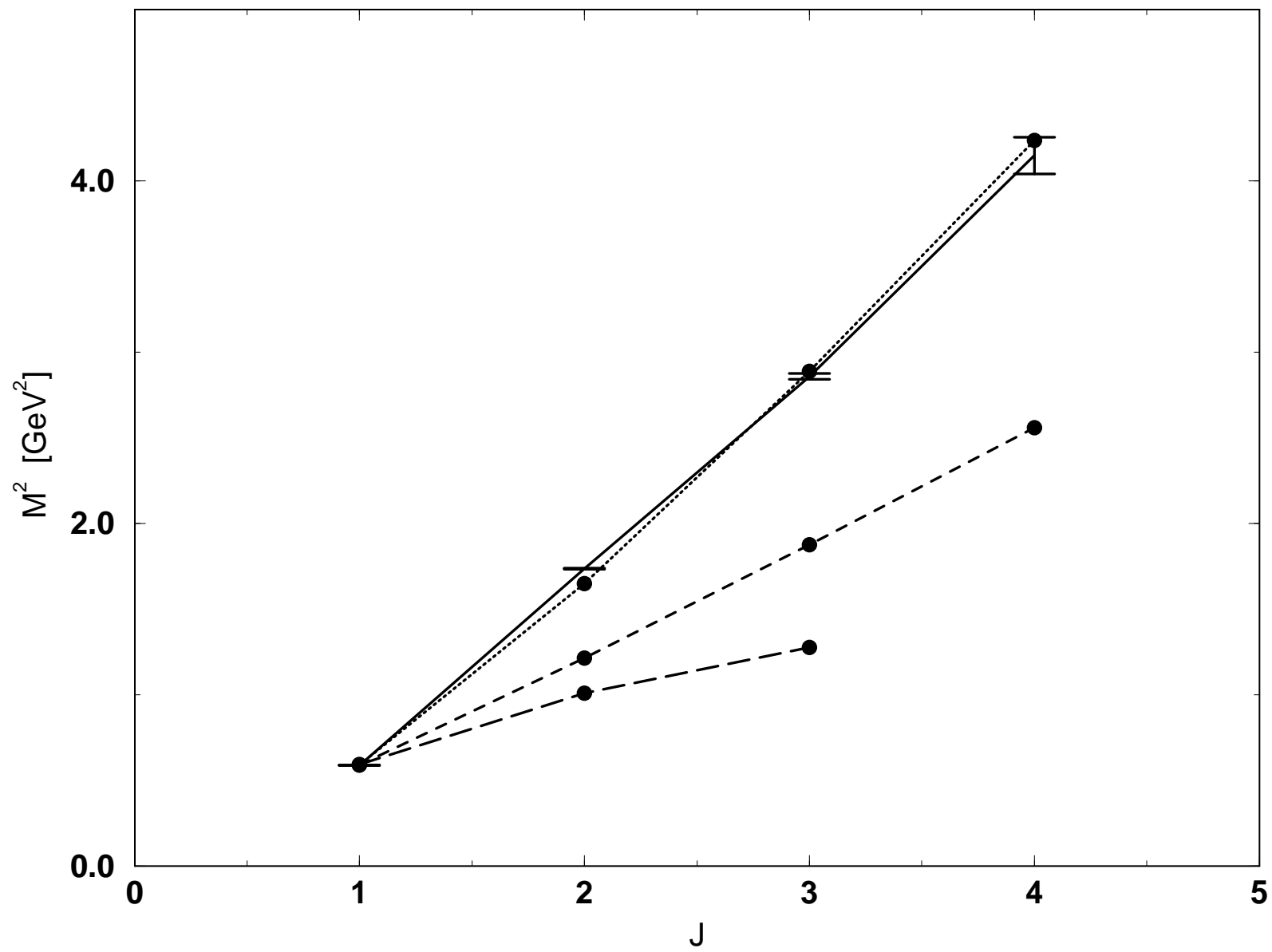


Fig.6

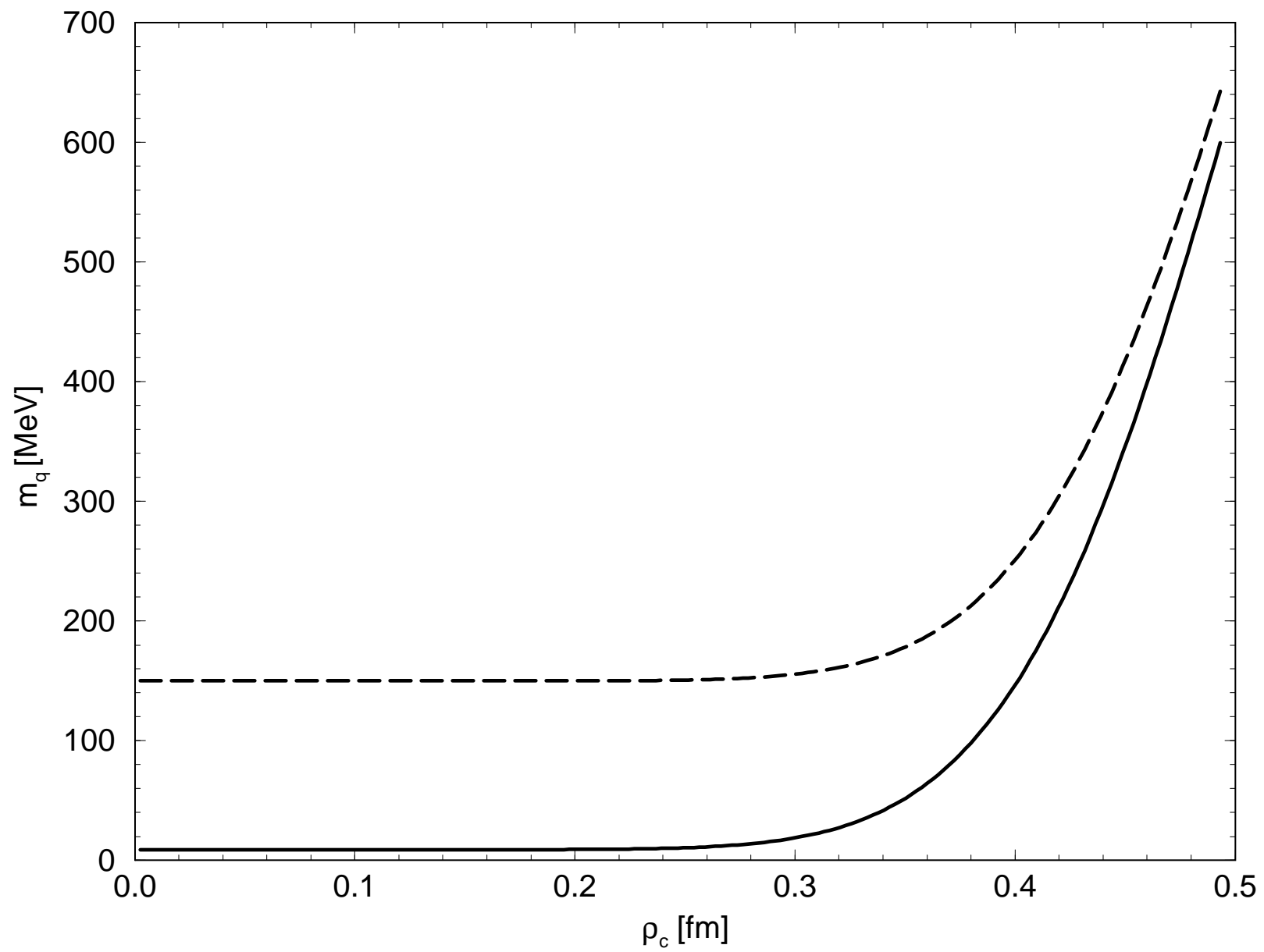


Fig.7

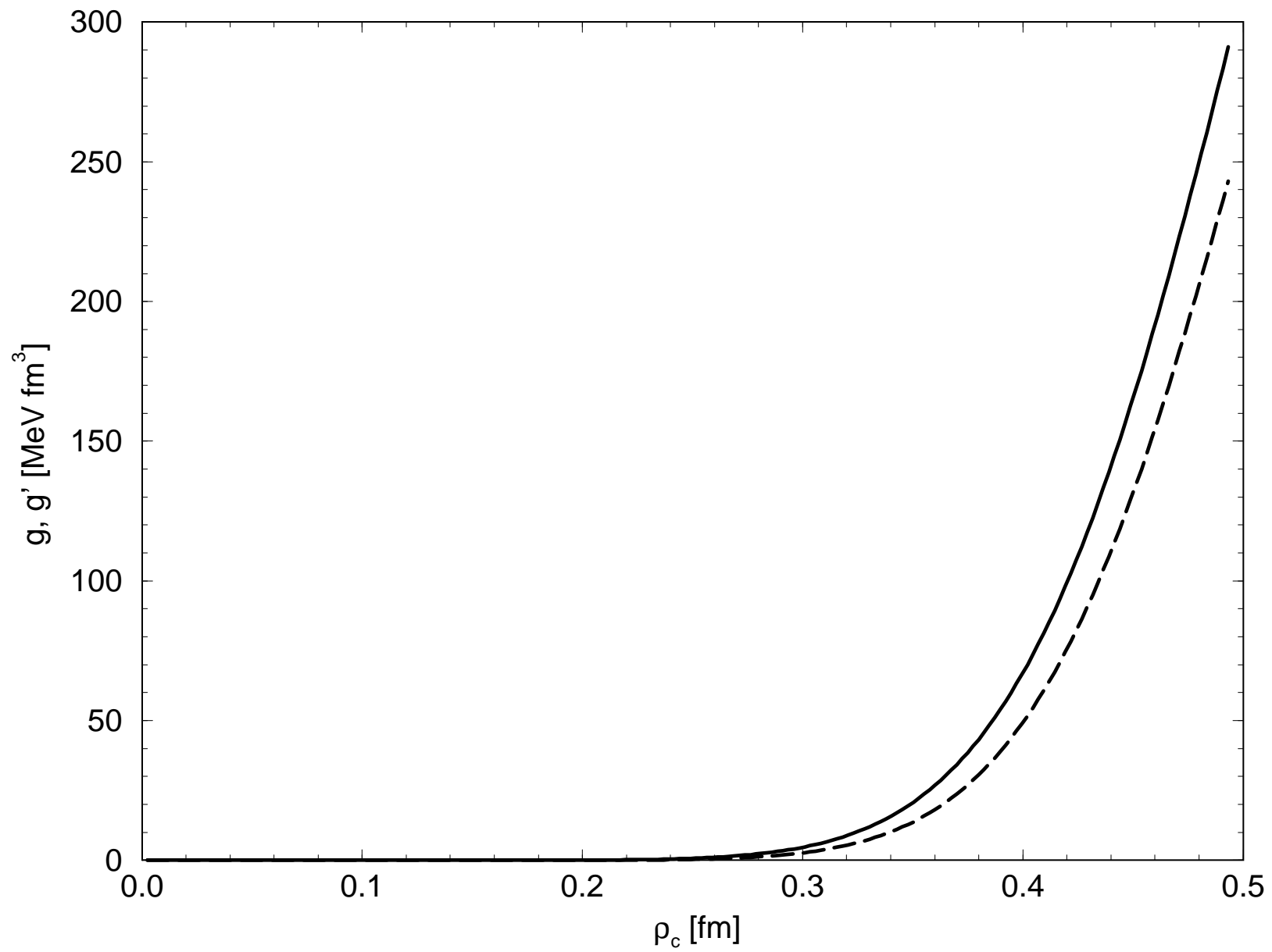


Fig.8

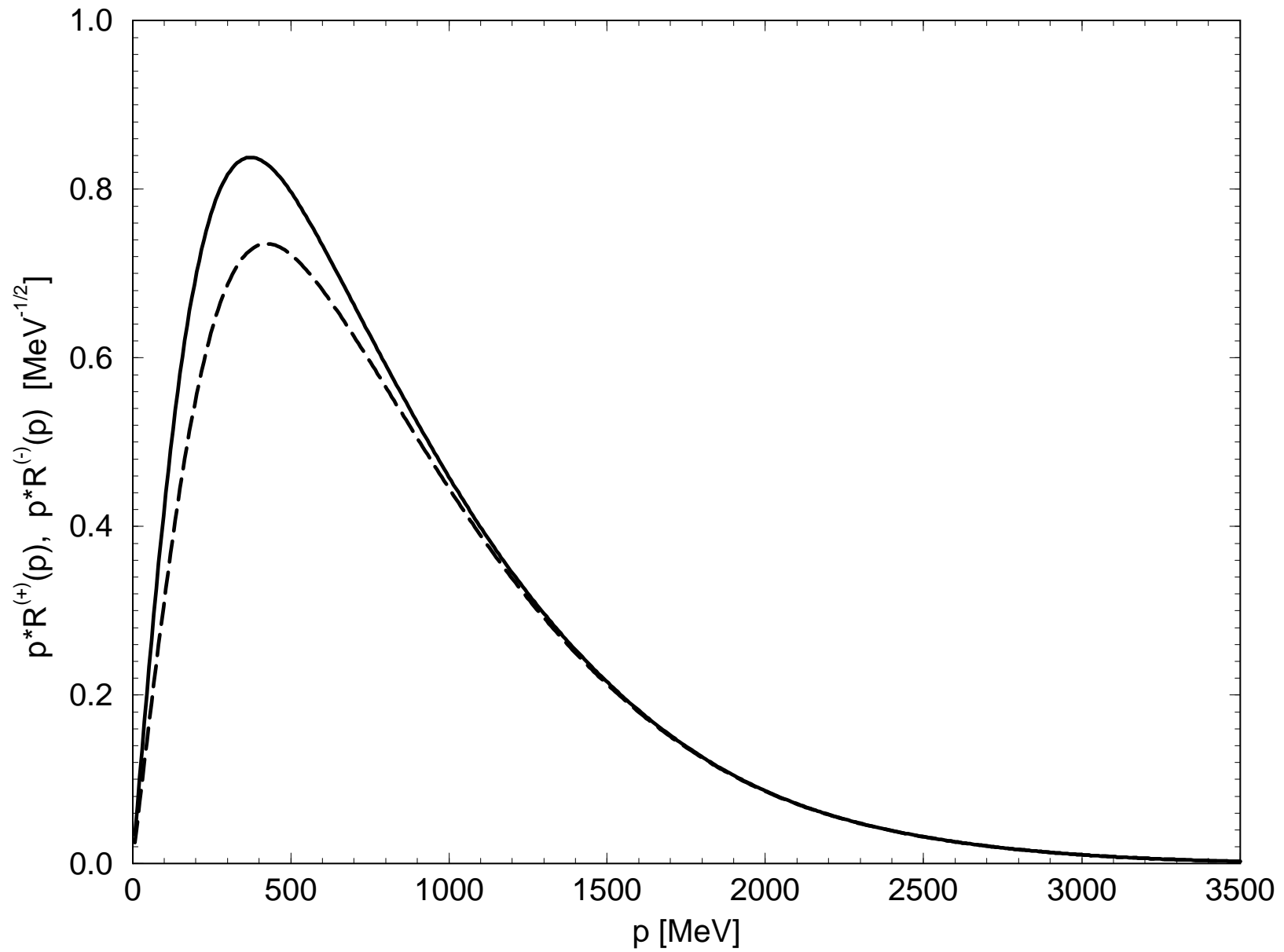


Fig.9

